Bremsstrahlung emission of high energy accompanying spontaneous fission of ^{252}Cf

S. P. Maydanyuk[*] and V. S. Olkhovsky[†]

Institute for Nuclear Research, National Academy of Science of Ukraine, Kiev 03680, Ukraine

G. Mandaglio, M. Manganaro, G. Fazio, and G. Giardina[‡]

Dipartimento di Fisica dell'Università di Messina, I-98166 Messina, Italy and Istituto Nazionale di Fisica Nucleare,
Sezione di Catania, I-95123 Catania, Italy

The study of the bremsstrahlung photon emission accompanying fragments produced in the spontaneous fission of heavy nuclei by a fully quantum approach is presented for the first time. This kind of problem requires the knowledge of wave functions of the fissioning system leading to a wide distribution of couples of fragments that are the products of fission. With the aim of obtaining these wave functions, the interaction potential between the emitted fragment and residual nucleus is calculated by a standard approach. A new procedure was performed that allows an increase in the accuracy of calculations of radial integrals in the far asymptotic region and the achievement of the convenient convergence in calculations of the spectra. The total probability of the emitted photons in the spontaneous fission of ^{252}Cf was calculated in such a way. We obtained good agreement between theory and experimental data up to 38 MeV for the bremsstrahlung spectrum of photons while the calculation of the total probability of photon emission accompanying fragments was performed up to an energy of 60 MeV. The analysis of contributions in the bremsstrahlung spectrum accompanying the emission of light, medium, and heavy fragments in the fission of ^{252}Cf is presented.

I. INTRODUCTION

Although modern models of nuclear decays in the determination of half-lives use semiclassical calculations of barrier penetrability [1–4], a quantum approach for the calculation of bremsstrahlung spectra accompanying such decays does not require the application of any semiclassical approximation. This advance opens an independent way (both theoretical and experimental) of obtaining new information on the decay and its dynamics. To achieve a satisfactory description of the bremsstrahlung emission accompanying the spontaneous fission of a heavy nucleus (for example, ^{252}Cf) where many kinds of fragments are involved, as a first step of our study we consider the fission emitting light fragments like ^{9}Be, ^{12}C, ^{24}Mg, and particularly the α decay from ^{252}Cf, to compare this last bremsstrahlung spectrum with the photon spectra found in the cases of ^{214}Po and ^{226}Ra nuclei.

In our previous paper [5], we studied the bremsstrahlung photon emission accompanying the α decay of heavy nuclei, and we found a relevant difference between the experimental bremsstrahlung spectra for the ^{214}Po and ^{226}Ra nuclei ($E_\alpha = 7.7$ MeV for ^{214}Po and $E_\alpha = 4.8$ MeV for ^{226}Ra); nevertheless, the α decay of such nuclei leads to very similar α-particle daughter nucleus potential (see Fig. 2 of Ref. [5]). We concluded that the different slopes of the spectra were connected with the different Q values of α decay for the two considered nuclei and we confirmed that such a difference gives different contributions of photon emission from the

tunneling region into the total spectrum. Moreover, because the photons are emitted more strongly when the α particle transits through the nuclear shape, we naturally came to the conclusion that the photon emission is also sensitive to the deformation of the nucleus.

Moreover, in Ref. [6] we showed that the photon emission probability during the α decay is sensitive to the direction of outgoing α particles with respect to the orientation of the symmetry axis of the deformed nucleus. So, we established a connection between the nuclear deformation $\beta_2 = 0.151$ and the bremsstrahlung spectrum accompanying the α decay of the ^{226}Ra nucleus.

Following the method used in Ref. [6] for the α decay, in the present article we develop a quantum approach to the case of bremsstrahlung photons emitted during spontaneous fission of a nucleus for which the bremsstrahlung spectrum is composed of a wide distribution of emitted fragments and daughter nuclei. In this case it is necessary to describe the daughter nucleus fragment potential by an appropriate model taking into account the different nuclear surface shapes of the nucleus undergoing fission for each of these combinations.

In Sec. II we present the generalized model of the bremsstrahlung spectrum of photons emitted during the spontaneous fission, and in Sec. III we give the results of the theoretical study for the ^{252}Cf nucleus. In Sec. IV we summarize the conclusions.

II. MODEL OF BREMSSTRAHLUNG EMISSION ACCOMPANYING THE SPONTANEOUS FISSION

A. Shape of the nuclear system undergoing fission

In the fission process it is necessary to describe the sequence of shapes of a fissioning nucleus from its ground state in a

---

[*]maidan@kinr.kiev.ua

[†]olkhovsk@kinr.kiev.ua

[‡]giardina@nucleo.unime.it

continuous way, through its saddle and scission configurations to the separated fragments at infinity. In a study of ground-state shapes, one has to be able to describe a sphere, oblate and prolate spheroids, octupole deformations, and positive and negative hexadecapole deformations. Because many questions studied in the fission process do not sensitively depend upon deviations from axial symmetry, we initially apply the model to shapes of nuclear systems that are axially symmetric.

We chose to specify the nuclear shape in terms of smoothly joined portions of three quadratic surfaces of revolution: two spheroids connected by a hyperboloidal neck (see Fig. 3 of Ref. [7]). In terms of the cylindrical coordinate system, we use the equation for the drop's surface written explicitly as [7]

$$\rho^2 = \begin{cases} a_1^2 - \left(a_1^2/c_1^2\right)(z-l_1)^2, & \text{for} \quad l_1 - c_1 \leqslant z \leqslant z_1, \\ a_2^2 - \left(a_2^2/c_2^2\right)(z-l_2)^2, & \text{for} \quad z_2 \leqslant z \leqslant l_2 + c_2, \\ a_3^2 + \left(a_3^2/c_3^2\right)(z-l_3)^2, & \text{for} \quad z_1 \leqslant z \leqslant z_2. \end{cases}$$
(1)

Here, the quantity l_i specifies the position of the center of the ith quadratic surface, c_i is its symmetry axis, and a_i is its transverse semiaxis ($i = 1, 2, 3$). There are nine coordinates in the specification of a nuclear shape. However, following the description reported in the article of Bolsterli *et al.* [7], one coordinate is eliminated by the assumption that the volume of the nuclear system remains constant during its evolution, and two other coordinates are eliminated by the requirement that the middle surface join smoothly with both surfaces of the forming fragments (at points denoted by z_1 and z_2). This introduces three relations between the original nine degrees of freedom and reduces the number to six. Elimination of the center-of-mass coordinate finally reduces the number of shape coordinates to five. As a demonstration of such a procedure applied for calculation of shapes with continuous deformation, in Fig. 1 we present the results of shapes obtained at different distances r between the centers of the daughter nucleus and the ^{12}C fragment (considered here as an example) formed in the process of fission of the ^{252}Cf nucleus. We use radii of the parent and daughter nuclei defined according to Ref. [8].
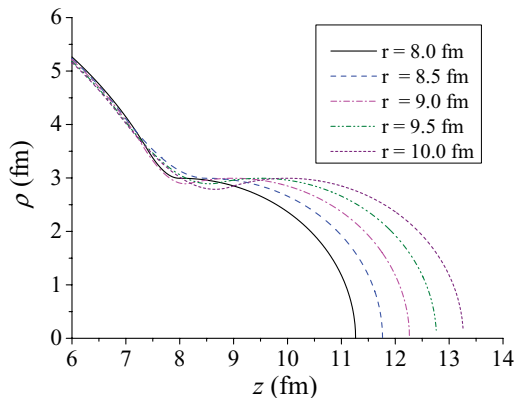

FIG. 1. (Color online) Shapes of the nuclear surface for emission of the ^{12}C fragment calculated for different distances r between centers of the daughter nucleus and the fragment during spontaneous fission of the ^{252}Cf nucleus [axes z and ρ are defined from Eq. (1)].

B. Interaction potential between the daughter nucleus and fragment

Once the nuclear shape has been specified, the next step is to generate an interaction potential between the daughter nucleus and fragment with respect to the shape and the distance between them. Over the years, considerable efforts were made to calculate the fissioning nucleus energy as a function of its neutron and proton numbers and its shape. If such a procedure is useful in the general theory of fission, it has to be capable of handling very deformed shapes and the evolution from one parent nucleus to two final fragments (the daughter nucleus and the related fission fragment). The interaction potential between the daughter nucleus and the fragment could be written as

$$V_{\text{total}}(\mathbf{r}) = V_C(\mathbf{r}) + V_N(\mathbf{r}).$$
(2)

The Coulomb component $V_C(\mathbf{r})$ describes electromagnetic interactions between daughter nucleus and fragment. We define this component as the energy formed by charges filling the volume of the fissioning system restricted by its shape (for details, see Ref. [7]). However, we suppose that the charge inside the volume of the fragment determines the energy of self-interactions caused by the distribution of the charges only inside this fragment and, so, it should not give its own contribution to the Coulomb component $V_C(\mathbf{r})$. Therefore, we can write the Coulomb component as

$$V_C(\mathbf{r}) = E_{C,\text{nucleus}}(\mathbf{r}) - E_{C,\text{fragment}},$$
(3)

where

$$E_{C,\text{nucleus}}(\mathbf{r}) = \lambda_C \int_{V,\,\mathbf{r} \neq \mathbf{r}'} \frac{\mathbf{dr'}^3}{|\mathbf{r}' - \mathbf{r}|},$$

$$E_{C,\text{fragment}} = \lambda_C \int_{V_f,\,r \neq 0} \frac{\mathbf{dr}^3}{|\mathbf{r}|}, \quad \lambda_C = \frac{Z_d\, Z_f\, e^2}{V_p}.$$
(4)

Here, we define the Coulomb energy of nuclear system $E_{C,\text{nucleus}}(\mathbf{r})$ like Eq. (3) in Ref. [7] but we use the generalized factor λ_C for the daughter and fragment charges during the spontaneous fission, where we take into account that the parent nucleus can be deformed. The Coulomb component of the fragment, $E_{C,\text{fragment}}$, is defined by a similar mode; however, we suppose that the shape and volume V_f of the fragment are fixed. The two integrals are over the volume V of the fissioning system (defined relative to the given distance r between centers of the daughter nucleus and fragment) and the volume V_f of the fragment, respectively; Z_d and Z_f are charges of the daughter nucleus and fragment, respectively. In Fig. 2(a), the Coulomb component (3) with Eq. (4) and Coulomb component from Ref. [1] calculated in the spherically symmetric approximation are presented for the α decay of the ^{252}Cf nucleus in comparison with the α decay of the ^{214}Po nucleus. As one can see, these two components are very close at higher distances r, whereas there is an appreciable difference at lower r values, for both considered systems.

We define the nuclear component $V_N(\mathbf{r})$ as the difference between the energy of the total nuclear system $E_{N,\text{nucleus}}(\mathbf{r})$ (at a given distance $\mathbf{r}$ between the daughter nucleus and fragment) and the nuclear energy $E_{N,\text{fragment}}$ of that fragment only as

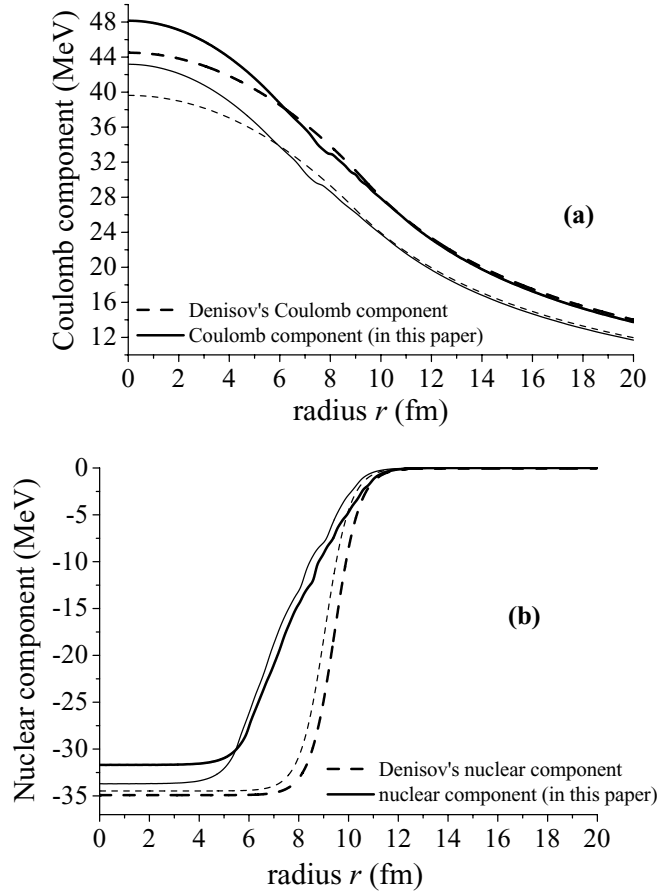$$V_N(\mathbf{r}) = E_{N,\text{nucleus}}(\mathbf{r}) - E_{N,\text{fragment}},$$
(5)

FIG. 2. Potential obtained in this article and spherically symmetric potential proposed by Denisov and Ikezoe in Ref. [1] for the α decay of the ^{252}Cf nucleus (thick lines) in comparison with the α decay of the ^{214}Po nucleus [5] (thin lines) for (a) the Coulomb components and (b) the nuclear components.

where $E_{N,\text{nucleus}}$ and $E_{N,\text{fragment}}$ can be written as

$$E_{N,\text{nucleus}}(\mathbf{r}) = -\lambda_N \int_V \frac{d\mathbf{r}^3}{1 + \exp(|\mathbf{r} - \mathbf{r}'|/a)},$$
$$E_{N,\text{fragment}} = -\lambda_N \int_{V_f} \frac{d\mathbf{r}^3}{1 + \exp(|\mathbf{r}|/a)}. \qquad (6)$$

The parameter $\lambda_N = M_p/V_p$ (where V_p and M_p are the volume and mass of the parent nucleus, respectively) practically gives a precise coincidence between the nuclear component defined by Eq. (5) with Eqs. (6) and the nuclear component obtained by the parametrization procedure proposed by Denisov and Ikezoe in Ref. [1] for the α decay. In Fig. 2(b), one can see that the nuclear components, studied for the α decay of ^{252}Cf in comparison with the α decay of ^{214}Po, are similar at the bottom (for distances shorter than 4 fm) and at the top (for distances longer than 10 fm) of the nuclear potential well, for both the decaying nuclei considered. Now, if we pass from our spherical symmetric approximation to the deformed variant of the potential used in Ref. [1], the difference between the two potentials becomes smaller. The analysis showed that the Yukawa folding functions (see, for example, Eq. (2) in Ref. [7]) do not give such an accurate coincidence as our functions in

Eq. (6), and so we use them for further calculations. The total potential depends on the difference between centers of the daughter nucleus and the emitted fragment, and we use the spherically symmetric approximation for further calculation of the wave functions.

The Q value concerning each emitted fragment in fission is calculated by standard procedure as

$$Q = M_p - M_d - M_f, \qquad (7)$$

where M_p, M_d, and M_f are the masses of the parent, daughter, and specific fragment nuclei, respectively. For the mass distribution of fragments we use the yields given in Ref. [9] in our calculation.

C. Model of bremsstrahlung accompanying a nuclear system decaying into two fragments

We define the photon emission probability caused by emission of a fragment during fission of a heavy nucleus in terms of the transition matrix elements for the composite quantum system (the daughter nucleus and fragment) from its state before the photon emission (initial state i) into its state after the photon emission (final state f). According to Eqs. (1) and (4) in Ref. [10] (see also Refs. [5,11,12]), we can write

$$\frac{dP(w, \vartheta_{f\gamma})}{dE_\gamma} = N_0 w |p(w, \vartheta_{f\gamma})|^2, \quad k_{i,f} = \sqrt{2m E_{i,f}},$$
$$w = E_i - E_f, \qquad (8)$$

where

$$p(w, \vartheta_{f\gamma}) = \sum_{\mu=-1,1} h_\mu \, \xi_\mu^* \int_0^{+\infty} r^2 \, dr$$
$$\times \int \psi_f^*(\mathbf{r}) \, e^{-ikr\cos\vartheta_{f\gamma}} \, \frac{\partial}{\partial \mathbf{r}} \, \psi_i(\mathbf{r}) \, d\Omega. \qquad (9)$$

Here, the vector $\mathbf{k}$ represents the photon impulse in the direction of its propagation, the vector $\mathbf{r}$ is the radius vector marking the position of the center of the emitted fragment relative to the center of the daughter nucleus, and $\vartheta_{f\gamma}$ is the angle between the direction $\mathbf{n}_1 = \mathbf{r}/r$ of the fragment motion (or tunneling) and the propagation direction $\mathbf{n}_2 = \mathbf{k}/k$ of the photon emitted, where $k = |\mathbf{k}|$ and $r = |\mathbf{r}|$. $E_{i,f}$ and $k_{i,f}$ are the total energy and wave vector of the system in the initial state i (i.e., the state before photon emission) or in the final state f (i.e., the state after photon emission), $\psi_i(\mathbf{r})$ and $\psi_f(\mathbf{r})$ are the wave functions of the system in the initial and final states i and f, $w = k = |\mathbf{k}|$ is the photon frequency (energy), and ξ_{-1} and ξ_{+1} are the vectors of the circular polarization with opposite rotation directions. We use the Coulomb calibration, where the polarization vectors $\mathbf{e}^{(\alpha)}$ for each photon are perpendicular to its wave vector $\mathbf{k}$. Moreover, we use the system of units where $\hbar = 1$ and $c = 1$. Such notations are used in accordance with Refs. [5,10–12]. N_0 is a coefficient calculated by (see Ref. [13])

$$N_0 = \frac{Z_{\text{eff}}^2 e^2}{(2\pi)^4 m}, \qquad (10)$$

where Z_{eff} and m are the effective charge and reduced mass of the daughter-fragment system, respectively, where

$Z_{\text{eff}} = (Z_f A_d - Z_d A_f)/(A_f + A_d)$ (symbols f and d represent fragment and daughter, respectively).

In a spherically symmetric approximation of the fissioning system, the matrix element (9) can be rewritten as

$$p(w, \vartheta) = -\sqrt{\frac{1}{3}} \sum_{l=0}^{+\infty} i^l (-1)^l (2l + 1) P_l(\cos \vartheta)$$
$$\times \sum_{\mu=-1,1} h_\mu J_{m_f}(l, w), \qquad (11)$$
$$h_\pm = \mp \frac{1}{\sqrt{2}}(1 \pm i).$$

Here, $J_{m_f}(l, w)$ is the radial integral independent of the angle ϑ:

$$J_{m_f}(l, w) = \int_0^{+\infty} r^2 R_f^*(r, E_f) \frac{\partial R_i(r, E_i)}{\partial r} j_l(kr) dr, \qquad (12)$$

where $R_i(r)$ and $R_f(r)$ are the radial components of the total wave functions $\psi_i(\mathbf{r})$ and $\psi_f(\mathbf{r})$ of the system in the initial state i and final state f, respectively; $j_l(kr)$ is the spherical Bessel function of order l; and $P_l(\theta)$ is Legendre's polynomial of order l. We use such selection rules for the quantum numbers l and m:

$$i \text{ state before emission:} \quad l_i = 0, \quad m_i = 0;$$
$$f \text{ state after emission:} \quad l_f = 1, \quad m_f = -\mu = \pm 1. \qquad (13)$$

To obtain the bremsstrahlung spectrum, we have to know wave functions (w.f.) in the initial and final states. We find the radial components $\chi_{i,f}(r)$ numerically on the basis of the given potential [here, $\chi_{i,f}(r) = r R_{i,f}(r)$], where the following boundary conditions should be used: before photon emission, we have the system with direct emission of the fragment, so the w.f. of such a system in the i state equals the outgoing plane wave at infinity; after photon emission, the state of the system could be changed and it is more convenient for the description of the f state to use w.f. for scattering of the fragment upon the daughter nucleus. So, we impose the following boundary conditions on the radial components $\chi_{i,f}(r)$:

$$\text{initial state } i: \quad \chi_i(r \to +\infty) \to G(r) + i F(r),$$
$$\text{final state } f: \quad \chi_f(r = 0) = 0, \qquad (14)$$

where F and G are the Coulomb functions as used in Ref. [1].

D. Calculation of the radial integrals in the far asymptotic region

Masses of heavy fragments participating in spontaneous fission of ^{252}Cf and high energies of emitted photons require that a large number of oscillations of integrand functions be taken into account. Serious problems arise concerning the fission in the bremsstrahlung spectra calculations. A fairly precise convergence in bremsstrahlung calculations can apparently be achieved with a determined mass region of fragments and photon energies if we can separate the integrand function forming the studied radial integral into different harmonics in the asymptotic region R_{as}. Then we integrated all these harmonics separately, and finally we reached the

total spectrum on the basis of such obtained integrals. So, using Eq. (12) for the radial integral, in the asymptotic region (starting from some value R_{as}) we have the following wave functions of the α-decaying nuclear system in the initial state i and final state f:

$$\psi_i(\mathbf{r}) = R_{i,l=0} Y_{00}(\mathbf{n}_r^i) = N_i \frac{G_{i,l=0}(r) + i F_{i,l=0}(r)}{r},$$
$$\psi_f(\mathbf{r}) = R_{f,l=1} \sum_m Y_{1m_f}(\mathbf{n}_r^f) \qquad (15)$$
$$= N_f \frac{A_f G_{f,l=1}(r) + B_f F_{f,l=1}(r)}{r} \sum_{m_f} Y_{1m_f}(\mathbf{n}_r^f),$$

where $F(r)$ and $G(r)$ are Coulomb functions, and we use the normalization

$$N_i = \sqrt{\frac{m}{k_i}}, \quad N_f = \frac{2}{\sqrt{A_f^2 + B_f^2}}. \qquad (16)$$

So, the asymptotic part of integral (12) can be written as

$$J_{\text{as}}(n) = N_i N_f \int_{R_{\text{as}}}^{R_{\text{max}}} [A_f G_f(r) + B_f F_f(r)] \frac{d}{dr}$$
$$\times \frac{G_i(r) + i F_i(r)}{r} j_n(k_{\text{ph}} r) r \, dr. \qquad (17)$$

After an appropriate elaboration of the formalism to obtain accurate formulas for the Coulomb functions in the far asymptotic region, we obtain the following expression for the asymptotic part of integral (12):

$$J_{\text{as}}(n)$$
$$= \frac{N_i N_f}{2} \int_{R_{\text{as}}}^{R_{\text{max}}} \left(k_i + \frac{i - \eta_i}{r} \right) [-(A_f - i B_f) \sin(\theta_i + \theta_f)$$
$$- (A_f + i B_f) \sin(\theta_i - \theta_f) + i(A_f - i B_f) \cos(\theta_i + \theta_f)$$
$$+ i(A_f + i B_f) \cos(\theta_i - \theta_f)] j_n(k_{\text{ph}} r) \, dr. \qquad (18)$$

For calculation of this integrand function see Appendix.

III. RESULTS

We applied the above-described method to calculate the spectrum of photons emitted during the spontaneous fission of the ^{252}Cf nucleus. To achieve this, we first needed to estimate in the bremsstrahlung spectrum the contribution from only one fragment (with the related daughter nucleus), with arbitrary mass and charge numbers A and Z, that is produced in the spontaneous fission process by a specific Q value. Figure 3(a) shows the distribution of Q values for fragments with mass number A included in the range 4–125 (more than 2000 fragments) in the spontaneous fission of ^{252}Cf. All these fragments cause specific emission of bremsstrahlung photons; therefore, the problem of obtaining the total bremsstrahlung spectrum in the spontaneous fission of a heavy nucleus is very complex.
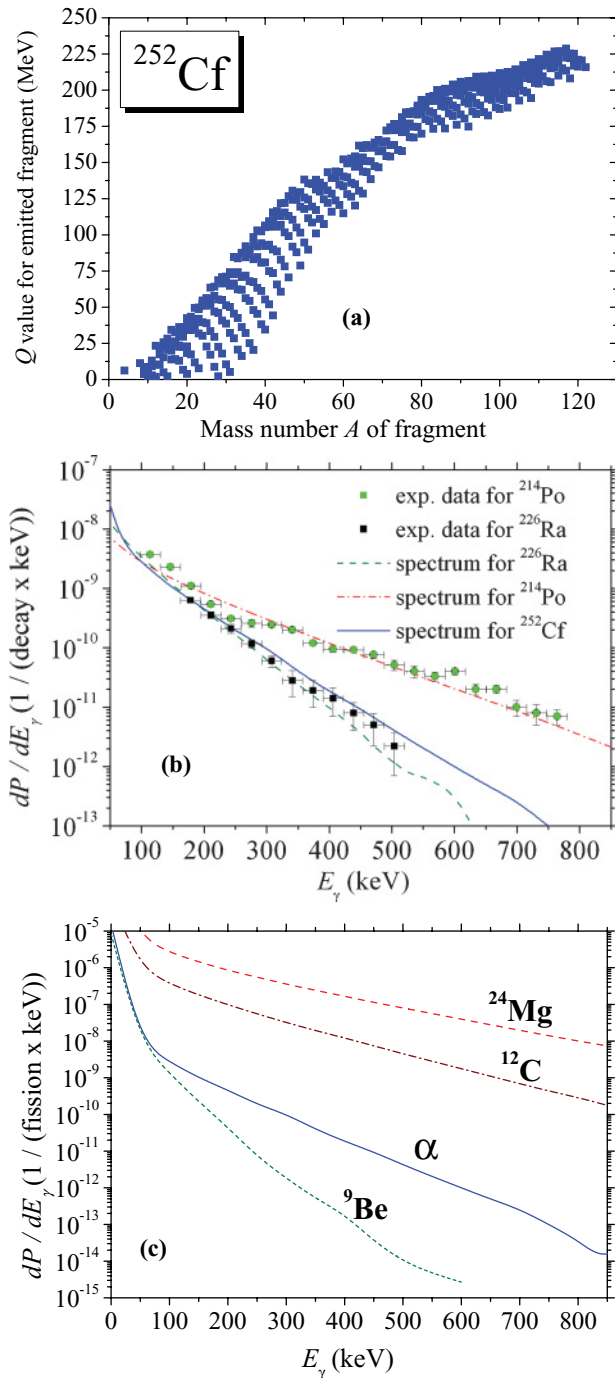
FIG. 3. (Color online) Bremsstrahlung probabilities obtained for light and medium fragments participating in fission of ^{252}Cf: (a) distribution of Q values relative to mass number A of fragments, which are emitted during the fission of the ^{252}Cf nucleus; (b) bremsstrahlung spectrum for the α emission from ^{252}Cf (solid line, $Q = 6.217$ MeV), in comparison with the spectra accompanying the α decay of ^{214}Po (dashed line, $Q = 7.7$ MeV) and ^{226}Ra (dash-dotted line, $Q = 4.8$ MeV), given in Ref. [5]; (c) bremsstrahlung spectra connected with the emission of ^{9}Be (dotted line, $Q = 6.927$ MeV), ^{12}C (dash-dotted line, $Q = 23.318$ MeV), and ^{24}Mg (dashed line, $Q = 54.583$ MeV) fragments from ^{252}Cf, in comparison with the bremsstrahlung spectrum for the α emission (solid line, $Q = 6.217$ MeV) from the same ^{252}Cf nucleus.

A. Emission caused by light and medium fragments in fission of ^{252}Cf

As a first step we selected this kind of fragment and calculated the spectrum of photons that we already know, as shown in the description of the bremsstrahlung emission during the α decay of heavy nuclei [5,6]. Also, in the present case of the ^{252}Cf nucleus, we started our calculations for the estimation of the bremsstrahlung spectrum accompanying the α decay. Results of such calculations are presented in Fig. 3(b), where we used $\vartheta_{\alpha\gamma} = 90°$ and $l = 0$. For a comparison we also included our previous results [5] for the α decay of the ^{214}Po and ^{226}Ra nuclei in this figure. The bremsstrahlung spectrum for the α emission from ^{252}Cf is lower than the one obtained for the α emission from ^{214}Po because the barrier for α emission is higher in the case of ^{252}Cf [see Fig. 4(a)]. As already noted in Fig. 2 of Ref. [5], the slope of photon emission is lower for the nucleus where the difference between the energy E_α and the top of barrier in the tunneling region is greater. As Fig. 4(a) shows, this also occurs for the α emission from ^{252}Cf. Moreover, in Fig. 3(c) we present the calculated photon spectra for the medium fragments, ^{9}Be, ^{12}C, and ^{24}Mg, in comparison with the photon spectrum obtained for the α decay from the same nucleus. The photon spectrum yield is higher for heavy fragments with higher Q values and effective charge. For the case of a bremsstrahlung spectrum connected with the emission of ^{9}Be from ^{252}Cf, the spectrum yield is lower than the one for the α emission because, in spite of the comparable Q values and effective charges [$Q(^9$Be$) = 6.927$ MeV, $Q(^4$He$) = 6.217$ MeV, and $Z_{\rm eff}(^9$Be$) = 0.5$, $Z_{\rm eff}(^4$He$) = 0.444$], the barrier for the ^{9}Be fragment in the tunneling region is larger than the one for the α emission [see Fig. 4(b)]. This condition for the ^{9}Be fragment decreases the emission probability of photons in comparison with the case of the α emission, as already observed in Ref. [5]. In the case of a heavier fragment, for example ^{24}Mg, the yield of the photon spectrum is higher than that for the lighter fragments.

B. Emission caused by heavy fragments and total spectrum of bremsstrahlung accompanying the spontaneous fission of ^{252}Cf

Calculations for photon emission accompanying heavy fragments are more complex. Fragments with larger masses determine fission events with larger Q values. To achieve stable bremsstrahlung spectra, we need to take a larger number of integrand function oscillations into account in the integration of the matrix element. High energies of emitted photons (from several hundreds of keV to tens of MeV) reinforce this difficulty. After explicit integration of the matrix element in the far asymptotic region, we improved our code to allow the achievement of the necessary stability for many heavy fragments. The results of such calculations for heavy fragments inside the region of masses $A = 95$–115 are presented in Fig. 5.

The total spectrum of photons emitted during the spontaneous fission of the ^{252}Cf nucleus is obtained by averaging the probabilities of photon emission from all separated fragments. The contribution of the photon emission caused by each fragment in the total bremsstrahlung spectrum is calculated by
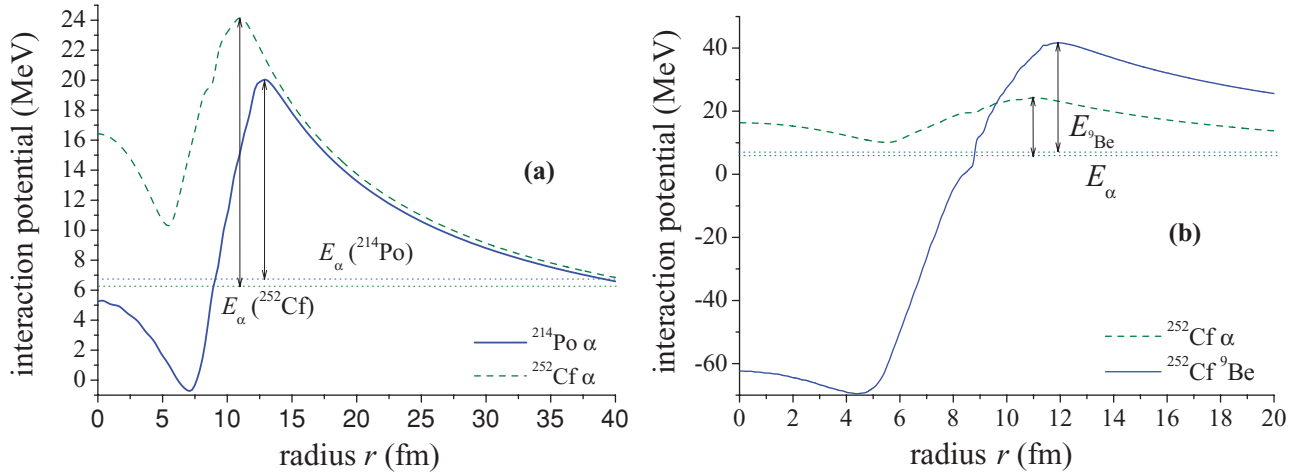
FIG. 4. (Color online) (a) The α nucleus barriers for the α decay from ^{252}Cf (dashed line) and ^{214}Po solid line): dotted lines represent the energy $E_\alpha = 6.217$ MeV for the α emission from ^{252}Cf, and the energy $E_\alpha = 6.7$ MeV for the α emission from ^{214}Po. (b) Barriers for the α emission (dashed line) from ^{252}Cf and the ^{9}Be fragment emission (solid line) from ^{252}Cf: dotted lines represent the energy $E_\alpha = 6.217$ MeV for the α emission from the ^{252}Cf, and the energy $E_{^9\text{Be}} = 6.927$ MeV for the ^{9}Be emission from the same nucleus. In both panels, the respective barriers are also indicated.

taking into account the fission probability of the ^{252}Cf nucleus for each fragment. So, we calculate the total bremsstrahlung spectrum by the formula

$$\frac{dP(w, \vartheta)}{dE_\gamma} = \sum_i a_i \frac{dP_i(w, \vartheta)}{dE_\gamma} \quad \left(\text{with the condition} \sum_i a_i = 1\right),$$

$$(19)$$

where a_i is the weight amplitude for the fission process emitting fragment with number i, and summation is performed over the involved region of masses. To find interesting weight amplitudes for different fragments, we used the mass distribution yields for the ^{252}Cf nucleus given in Ref. [14] in comparison with the experimental data [15]. Because the main region of the fragment distribution is contributed by fragments of spontaneous fission included in the 95–115 mass range (with daughter nuclei included in the complementary 137–157 range), we limited our calculation of the bremsstrahlung emission within this fragment range. As an example, in Fig. 5(a) we present the comparison of the bremsstrahlung probability related to the photon emission accompanying the spontaneous fission of ^{252}Cf by seven fragments (from ^{95}Zr to ^{115}Rh) with masses included in the above-mentioned region.

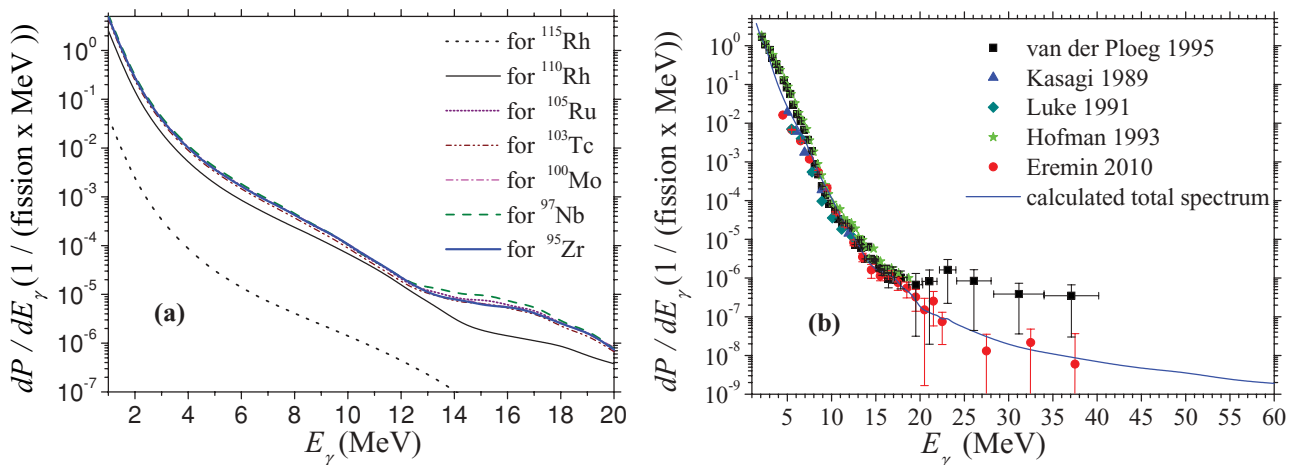FIG. 5. (Color online) (a) Calculation of bremsstrahlung photon emission probabilities caused by heavy fragments included in mass region $A = 95$–115 during the spontaneous fission of the ^{252}Cf nucleus (solid line, ^{95}Zr fragment: $Q = 202.36$ MeV, $Z_{\text{eff}} = 3.055$; dashed line, ^{97}Nb: $Q = 200.43$ MeV, $Z_{\text{eff}} = 3.277$; dash-dotted line, ^{100}Mo: $Q = 204.81$ MeV, $Z_{\text{eff}} = 3.111$; dashed double-dotted line, ^{103}Tc: $Q = 204.47$ MeV, $Z_{\text{eff}} = 2.944$; short dotted line, ^{105}Ru: $Q = 205.22$ MeV, $Z_{\text{eff}} = 3.166$; thin solid line, ^{110}Rh: $Q = 214.53$ MeV, $Z_{\text{eff}} = 2.222$; dotted line, ^{115}Rh: $Q = 226.74$ MeV, $Z_{\text{eff}} = 0.277$). (b) Total bremsstrahlung photon probability in the spontaneous fission of the ^{252}Cf nucleus: calculation of the spectrum (solid line) obtained by averaging the spectra for contributions of all fragments; sets of experimental data given by squares [16], triangles [17], diamonds [18], stars [19], and circles [20].

The different contributions of bremsstrahlung probability of various fragments are sensitive to the effective charge Z_{eff} and the Q value of each decay fragment. While for many considered fragments the Q values and Z_{eff} are substantially comparable and the contributions of photon emission are comparable too, for the case of the ^{115}Rh fragment, Z_{eff} is very low (0.277) and the bremsstrahlung spectrum contribution is lower than the others. Figure 5(b) shows the average total spectrum (solid line) of the photon emission probability calculated by formula (19). In Fig. 5(b) we also include as a comparison the experimental data given in various papers [16–19] and Ref. [20]. Our calculations were obtained in the framework of a fully quantum approach and agree well with the experimental data in the literature concerning bremsstrahlung photon emission in the spontaneous fission of ^{252}Cf in the E_γ energy range up to about 20 MeV. In the 20–38-MeV range, however, the calculations agree only with the experimental data of Eremin *et al.* [20].

At the conclusion of this section we briefly discuss the possibility of investigating the influence on the bremsstrahlung spectrum of photon emission during spontaneous fission if one includes in the liquid drop model (i) variations due to the charge distribution inside the nuclear system and its motion during the dynamics of the fissioning process and (ii) the effects of the shell corrections on the density inside the nuclear system and the fission barrier.

Such aspects can constitute an interesting prospective of investigating eventual relevant modifications of the bremsstrahlung spectra, because the inclusion of the mentioned details should be reflected in some modifications of the interaction potential between the daughter nucleus and the emitted fragment, which could appear in the bremsstrahlung spectrum. At the present status of our proposed model, the influence of such proposed modifications to the bremsstrahlung spectra seems to be smaller than the present achieved accuracy of the calculated spectra. For example, if we shift the boundary of the asymptotic region R_{as} to smaller values, where we apply the approach presented in Sec. II D and Appendix, the error that appears after such a shift is smaller than the error that we have in direct calculation of the matrix element based on the wave functions obtained separately by our more accurate and nonasymptotic method. Moreover, the considered boundary is in the external region of Coulomb forces, where the emission seems to be stronger, while aspects of the liquid drop model take place in the nuclear region. So, if we want to study the effects caused by peculiarities of the liquid drop model, at first we have to solve the above-mentioned technical problems to obtain convergent spectra. In any case, in spite of the difficulty in teh form of complex and long calculation times, the modification of the interaction potential including variations of the nuclear density in the framework of the modern liquid drop model and shell corrections (see, for example, Refs. [21–24]) is an interesting prospective task.

IV. CONCLUSIONS

In this article we presented a new development of our model concerning the study of the bremsstrahlung photon emission accompanying the spontaneous fission of heavy nuclei, for example, ^{252}Cf. We studied the fissioning process in a fully quantum approach using the spherical wave approximation for the description of a photon wave function (see Ref. [25]). We applied our method to the spontaneous fission of the ^{252}Cf nucleus and checked the model and calculation by experimental data [16–20] for the fission of ^{252}Cf. Our results on the total bremsstrahlung spectrum probability calculated up to about $E_\gamma = 60$ MeV of photon emission accompanying the spontaneous fission of ^{252}Cf were in good agreement with the experimental data of Eremin *et al.* [20] given up to about $E_\gamma = 38$ MeV, whereas in the $E_\gamma = 20$–38 MeV energy range the data of van der Ploeg *et al.* [16] differed on average by a factor of 10 in comparison with our results and the data of Ref. [20]. We analyzed the photon spectra for light, medium, and heavy fragments produced in the ^{252}Cf fission and we observed the connection between the yield of the bremsstrahlung spectrum due to each fragment, the related Q value, and the effective charge Z_{eff}, which determine the wave functions of the fissioning system and the bremsstrahlung emission probability. To obtain these wave functions, we used the interaction potential between the emitted fragment and residual (daughter) nucleus calculated by a standard approach. One of the main problems was the calculation of the radial integrals that form the matrix elements of emission. We performed a new procedure which allows us to essentially increase the accuracy of wave-function calculation in far asymptotic regions. Such a new procedure has provided the possibility to study for the first time the bremsstrahlung photon emission in the fission problem in the fully quantum approach and to calculate the γ-spectrum probability up to $E_\gamma = 60$ MeV for the ^{252}Cf spontaneous fission.

Moreover, we think that the inclusion of more details in the liquid drop model to study its effects on the bremsstrahlung spectra of photon emission, in spite of the difficulties of complex and long calculation times, is an interesting prospective task.

APPENDIX: CALCULATION OF THE INTEGRAND FUNCTION

In Fig. 6(a) we present the calculation of the integrand function by formula (18). As one can see, this function appears to be quite complicated and has a harmonic structure. By analyzing its behavior in more detail we find that this function has a huge number of oscillations. In Fig. 6(b), we report the concrete calculation obtained for the range of radius r of 1 fm (from 890 to 891 fm) in the case of the ^{115}Rh fragment emitted from the fission of ^{252}Cf, and for photons in a 300-keV energy range. The function has about 8 oscillations in this range of 1 fm, whereas inside the 25–2225 fm region it has 17 600 oscillations.

However, integral (18) can be separated explicitly into integrals based on different harmonics:

$$J_{\mathrm{as}}(n) = \frac{N_i N_f k_i}{2}[-(A_f - i B_f)J_1^+ - (A_f + i B_f)J_1^- \\ + i(A_f - i B_f)J_2^+ + i(A_f + i B_f)J_2^-]$$
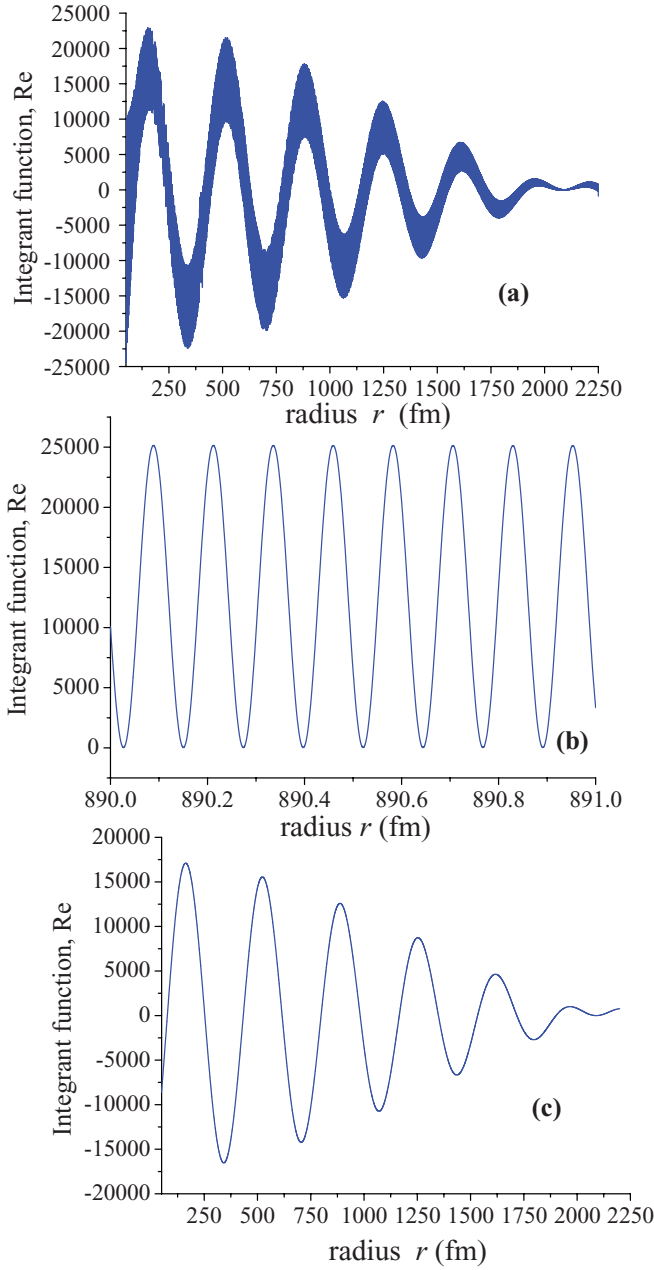
FIG. 6. (Color online) (a) Real part of the integrand function of the radial integral (17) for the ^{115}Rh fragment emitted during spontaneous fission of the ^{252}Cf nucleus; (b) shape of this function inside 1 fm (from 890 up to 891 fm), where one can see that this function has about eight oscillations; (c) integrand function of integral (A3), representing the harmonic approximation of original integral (18).

$$+ \frac{N_i N_f(i - \eta_i)}{2}[-(A_f - i B_f)J_3^+ - (A_f + i B_f)J_3^-$$
$$+ i(A_f - i B_f)J_4^+ + i(A_f + i B_f)J_4^-], \tag{A1}$$

where

$$J_1^\pm(n) = \int_{r_{as}}^{r_{max}} \sin(\theta_i \pm \theta_f) j_n(k_{ph}r) \, dr,$$

$$J_2^\pm(n) = \int_{r_{as}}^{r_{max}} \cos(\theta_i \pm \theta_f) j_n(k_{ph}r) \, dr,$$

$$J_3^\pm(n) = \int_{r_{as}}^{r_{max}} \sin(\theta_i \pm \theta_f) \frac{j_n(k_{ph}r)}{r} \, dr,$$

$$J_4^\pm(n) = \int_{r_{as}}^{r_{max}} \cos(\theta_i \pm \theta_f) \frac{j_n(k_{ph}r)}{r} \, dr. \tag{A2}$$

With the aim of finding integrals with the largest period of oscillations of the integrand functions, we should use harmonics with the smallest argument; that is, we obtain $\theta_i - \theta_f$ and the J_1^-, J_2^-, J_3^-, J_4^- integrals. The integrand functions in J_3^- and J_4^- decrease more strongly at increasing r in comparison with the ones in J_1^- and J_2^-. So, J_3^- and J_4^- have smaller contributions in the total integral (A1). Therefore, formula (A1) can be written in a simplified form:

$$J_{as}^-(n) \cong \frac{N_i N_f k_i}{2}(A_f + i B_f)[-J_1^-(n) + i J_2^-(n)]. \tag{A3}$$

In Fig. 6(c), we present the integrand function of this integral. Comparing it with the integrand function of the total integral presented in Fig. 6(a) we conclude that the integrand function of J_{as}^- tends to the original function, but already without oscillations, which seriously decreases its convergence. So, integral (A3) can be considered an acceptable approximation of the previous integral. In particular, inside the considered region from $r = 25$ fm up to $r = 2225$ fm, we obtain only 6 oscillations for the integral $J_{as}^-(0)$, in comparison with 17 600 oscillations for the previous integral, $J_{as}(0)$. The two integrals J_3^+ and J_4^+ seem to give further corrections to the total integral. Therefore, we define the following integral as

$$J_{as}^+(n) \cong \frac{N_i N_f k_i}{2}(A_f - i B_f)[-J_1^+(n) + i J_2^+(n)]. \tag{A4}$$

Moreover, as a last correction, taking into account the greater decreasing speed of the integrand function at increasing r, we can write the following:

$$J_{as}^{(r)}(n) \cong \frac{N_i N_f k_i}{2}\{(A_f + i B_f)[-J_3^-(n) + i J_4^-(n)]$$
$$+ (A_f - i B_f)[-J_3^+(n) + i J_4^+(n)]\}. \tag{A5}$$

Of course, the summation of these integrals gives the initial integral (A3) exactly. Our calculations of the bremsstrahlung spectra for different heavy fragments showed that corrections on the basis of $J_{as}^+(n)$ and $J_{as}^{(r)}(n)$ are practically small, so the leading approximation provides very good accuracy.

If we want to include the contribution at $r > r_{max}$ in our consideration, we should further improve calculations of the total radial integrals. To this aim, we use the following approximated formulas:

$$\int_{r_{max}}^{+\infty} \frac{\cos \alpha r \, dr}{r} = \left. \frac{\sin \alpha r}{\alpha r} \right|_{r_{max}}^{+\infty} + \int_{r_{max}}^{+\infty} \frac{\sin \alpha r \, dr}{\alpha r^2}$$
$$\simeq -\frac{\sin \alpha r_{max}}{\alpha r_{max}} + O(r_{max}^{-2}),$$

$$\int_{r_{max}}^{+\infty} \frac{\sin \alpha r \, dr}{r} = \left. -\frac{\cos \alpha r}{\alpha r} \right|_{r_{max}}^{+\infty} - \int_{r_{max}}^{+\infty} \frac{\cos \alpha r \, dr}{\alpha r^2}$$
$$\simeq \frac{\cos \alpha r_{max}}{\alpha r_{max}} + O(r_{max}^{-2}), \tag{A6}$$

which have an accuracy up to r_{max}^{-2}. For the first $n = 0$, we obtain

$$
\begin{aligned}
J_{1,\text{rest}}^{-}(0) \simeq \frac{N_i N_f k_i}{4k_{\text{ph}}} \Bigg[&(A_f + i B_f) \frac{\sin(\theta_i - \theta_f - k_{\text{ph}} r)}{(k_i - k_f - k_{\text{ph}})r} \\
&- (A_f + i B_f) \frac{\sin(\theta_i - \theta_f + k_{\text{ph}} r)}{(k_i - k_f + k_{\text{ph}})r} \\
&+ (B_f - i A_f) \frac{\cos(\theta_i - \theta_f - k_{\text{ph}} r)}{(k_i - k_f - k_{\text{ph}})r}
\end{aligned}
$$

$$
\begin{aligned}
&\left. - (B_f - i A_f) \frac{\cos(\theta_i - \theta_f + k_{\text{ph}} r)}{(k_i - k_f + k_{\text{ph}})r} \right] \Bigg|_{r=r_{max}} \\
&+ O\left(r_{max}^{-2}\right).
\end{aligned}
\tag{A7}
$$

Other integrals for the next n can be calculated in this way. However, our estimations show a negligibly small role of all such integrals $J_{i,\text{rest}}^{\pm}(n)$, if the leading integral J_{as}^{-} is calculated by formula (A3) correctly and the value of r_{max} is selected in an appropriate way.

[1] V. Yu. Denisov and H. Ikezoe, Phys. Rev. C **72**, 064613 (2005).

[2] B. Buck, A. C. Merchant, and S. M. Perez, At. Data Nucl. Data Tables **54**, 53 (1993).

[3] S. Åberg, P. B. Semmes, and W. Nazarewicz, Phys. Rev. C **56**, 1762 (1997).

[4] A. Sobiczewski and K. Pomorski, Prog. Part. Nucl. Phys. **58**, 292 (2007).

[5] G. Giardina, G. Fazio, G. Mandaglio, M. Manganaro, S. P. Maydanyuk, V. S. Olkhovsky, N. V. Eremin, A. A. Paskhalov, D. A. Smirnov, and C. Saccá, Mod. Phys. Lett. A **23**, 2651 (2008).

[6] S. P. Maydanyuk, V. S. Olkhovsky, G. Giardina, G. Fazio, G. Mandaglio, and M. Manganaro, Nucl. Phys. A **823**, 38 (2009).

[7] M. Bolsterli, E. O. Fiset, J. R. Nix, and J. L. Norton, Phys. Rev. C **5**, 1050 (1972).

[8] G. Royer, Nucl. Phys. A **807**, 105 (2008).

[9] G. Audi, A. H. Wapstra, and C. Thibault, Nucl. Phys. A **729**, 337 (2003).

[10] S. P. Maydanyuk and V. S. Olkhovsky, Eur. Phys. J. A **28**, 283 (2006).

[11] G. Giardina, G. Fazio, G. Mandaglio, M. Manganaro, C. Saccá, N. V. Eremin, A. A. Paskhalov, D. A. Smirnov, S. P. Maydanyuk, and V. S. Olkhovsky, Eur. Phys. J. A **36**, 31 (2008).

[12] S. P. Maydanyuk and V. S. Olkhovsky, Prog. Theor. Phys. **109**, 203 (2003).

[13] S. P. Maydanyuk, Open Nucl. Part. Phys. J. **2**, 1 (2009).

[14] Z. Büyükmumcu and M. Kildir, Phys. Rev. C **74**, 054613 (2006).

[15] C. Budtz-Jorgensen and H.-H. Knitter, Nucl. Phys. A **490**, 307 (1988).

[16] H. van der Ploeg, J. C. S. Bacelar, A. Buda, C. R. Laurens, and A. van der Woude, Phys. Rev. C **52**, 1915 (1995).

[17] J. Kasagi *et al.*, J. Phys. Soc. Jpn. Suppl. **58**, 620 (1989).

[18] S. J. Luke, C. A. Gossett, and R. Vandenbosch, Phys. Rev. C **44**, 1548 (1991).

[19] D. J. Hofman, B. B. Back, C. P. Montoya, S. Schadmand, R. Varma, and P. Paul, Phys. Rev. C **47**, 1103 (1993).

[20] N. V. Eremin *et al.*, Int. J. Mod. Phys. E **19**, 1183 (2010).

[21] V. M. Strutinsky, Nucl. Phys. A **95**, 420 (1967).

[22] M. Brack, J. Damgaard, A. S. Jensen, H. C. Pauli, V. M. Strutinsky, and C. Y. Wong, Rev. Mod. Phys. **44**, 320 (1972).

[23] F. A. Ivanyuk and K. Pomorski, Phys. Rev. C **79**, 054327 (2009).

[24] H. Hofmann and F. A. Ivanyuk, Phys. Rev. Lett. **90**, 132701 (2003).

[25] S. P. Maydanyuk and S. V. Belchikov, Probl. At. Sci. Technol. **5**, 19 (2004).